



Thermoanalytical and spectroscopic characteristics of young and old leaves powder and methanolic extracts of *Niedenzuella multiglandulosa*

Helena Mannocho Russo¹ · Wilhan Donizete Gonçalves Nunes¹ · Vanderlan da Silva Bolzani¹ · Massao Ionashiro¹ · Flávio Junior Caires^{1,2}

Received: 17 October 2017 / Accepted: 19 December 2017 / Published online: 2 January 2018

© Akadémiai Kiadó, Budapest, Hungary 2018

Abstract

Niedenzuella multiglandulosa is a plant species known for having high toxicity and to cause death in cattle and sheep, promoting economic losses in Brazilian trade balance difficult to estimate. This work aims to evaluate the potential of thermoanalytical techniques (TG–DSC, TG-FTIR) and FTIR to identify compositional differences between the powder samples and methanolic extracts of young and old leaves. The TG–DSC profile for young and old leaves powder and extract presented some differences, mainly in the fourth mass loss step, that was attributed to the greater content of tannins in old leaves as also evidenced by FTIR. The cyclic DSC and TG curves showed that the leaves samples are highly hygroscopic, adsorbing water vapor even from the controlled humidity atmosphere. This characteristic thermal behavior can be useful for sample identification and characterization.

Keywords *Niedenzuella multiglandulosa* · Thermal analysis · Evolved gas analysis · Natural products

Introduction

Niedenzuella multiglandulosa A. Juss. (Malpighiaceae), popularly known in Brazil as “cipó-vermelho” (red-vine) or “cipó-ferro” (iron-vine), formerly called *Tetrapteryx multiglandulosa* [1], is a shrub species or vine, found in the Brazilian states of Rio de Janeiro, São Paulo and Mato Grosso do Sul [2]. This species is known for presenting high toxicity, leading to chronic intoxication in cattle and sheep when ingested, and might cause death of these animals in weeks or months [3]. Consequently, these plants can cause economic losses in Brazilian trade balance that are difficult to estimate, once its economy is highly dependent on livestock.

The chemical composition of young and old leaves is known to be different, as found by an ongoing (unpublished) study. However, the main technique employed to identify composition differences between these samples is high-performance liquid chromatography (HPLC), which is time-consuming, requires several extraction steps with different polarity solvents and consequently generates residues that are an environmental issue. The thermoanalytical techniques can overcome most of these issues, because it is fast, requires minute sample amounts, and can be considered a green technique. Also, to the best of our knowledge, few studies employed thermoanalytical techniques in the characterization of plants dried leaves as a fingerprint method to identify samples [4–7].

The main objective of this work was to use the thermoanalytical techniques to characterize the dried leaves and extracts of plant leaves. For this, young and old leaves powders as well as its methanolic extracts were studied by means of thermoanalytical methods (TG–DSC, DSC, EGA/TG-FTIR) and infrared spectroscopy as a potential method to identify compositional differences between the samples. The thermal behavior and curve profile obtained in thermal analysis by TG–DSC and DSC can be used as a fingerprint for a specific sample, whereas FTIR can be used to identify

Helena Mannocho Russo and Wilhan Donizete Gonçalves Nunes have contributed equally to this work.

✉ Flávio Junior Caires
caires.flavio@fc.unesp.br

¹ Instituto de Química, Universidade Estadual Paulista (Unesp), Araraquara, SP, Brazil

² Faculdade de Ciências, Universidade Estadual Paulista (Unesp), Bauru, SP, Brazil

different compositions by analysis of the functional groups present. The identification of gases evolved during thermal degradation is also of great value, once they are directly correlated with the sample composition.

Materials and methods

N. multiglandulosa leaves (young and old) were collected in Mato Grosso do Sul State in November 2015, Campo Grande city, Brazil, by Prof. Nilton Carvalho from the Federal University of Mato Grosso do Sul. A voucher specimen (HMS5206) was deposited at the “Herbarium of Mato Grosso do Sul” from EMBRAPA Campo Grande, Mato Grosso do Sul, Brazil.

The leaves were firstly shade dried, transferred to an oven at 50 °C for 72 h, and then shredded in a knife mill. For the thermal analysis, the powders were sieved through a 0.30-mm mesh to normalize the particle size. The leaves were also extracted with methanol by maceration (24 h, 3 times) after being submitted to the same process with chloroform, hexane and ethyl acetate. Young leaves methanolic extract was chosen for this study as it was found to be the most toxic in an in vivo Zebrafish toxicity assay (unpublished).

Simultaneous thermogravimetry–differential scanning calorimetry (TG–DSC) curves were measured in a Mettler Toledo’s TG/DSC1 thermal analysis system. Samples weighing 10 mg were placed in 70- μ L α -alumina crucibles and heated from 30 to 1000 °C under compressed dry air atmosphere (50 mL min⁻¹), at a heating rate of 10 °C min⁻¹.

Differential scanning calorimetry (DSC) experiments were performed in a TA Instruments model Q10 calorimeter. Samples weighing 2.0 mg were placed in aluminum pans with perforated lids and heated from 30 to 180 °C, under compressed dry air atmosphere at 50 mL min⁻¹ flow rate, and 10 °C min⁻¹ heating rate. A similar empty pan with perforated lid was used as reference material.

Gases evolved during thermal analysis of the sample were identified by coupling the TG–DSC to a Nicolet’s iS10 infrared spectrometer (TG–FTIR). It was done by a transfer line (120 cm), heated at 225 °C to avoid condensation of the evolved gaseous products. The spectrometer was equipped with a heated (250 °C) cell gas, with a DTGS detector and KBr windows. Spectra acquisition was made at 16 scans per spectrum, and 4 cm⁻¹ resolution.

Infrared absorption spectroscopy of the powder and extract samples was performed in the same spectrometer, although in this case it was equipped with an ATR accessory, with Ge crystal as sample support. Spectra were collected with 32 scans per spectrum, at 4 cm⁻¹ resolution.

Results and discussion

Simultaneous thermogravimetry–differential scanning calorimetry (TG–DSC)

Young (YL) and old leaves (OL) powder

In Fig. 1 it is shown the TG–DSC/DTG curves for the *N. multiglandulosa* young (YL) and old (OL) leaves, respectively. These curves are very similar, although some differences can be observed.

The first mass loss observed from 30 to 132 °C (YL, 7.10%) and 30–133 °C (OL, 8.04%), both with a wide endotherm in the same temperature range in the DSC curve, can be attributed to the loss of adsorbed/superficial water, once this step initiates at low temperature. However, the second mass loss from 132 to 172 °C (YL, 1.86%) and 133–173 °C (OL, 2.21%) is associated with more pronounced endothermic events in the DSC curve, especially in the OL sample, and could be attributed to elimination of constitutional water molecules. The figure insets (red stars) help to better visualize these aspects of DSC curve. Also, for the second step of OL sample the DTG curve shows an evidence of two superposed mass losses, suggesting a different process of dehydration when compared to YL leaves.

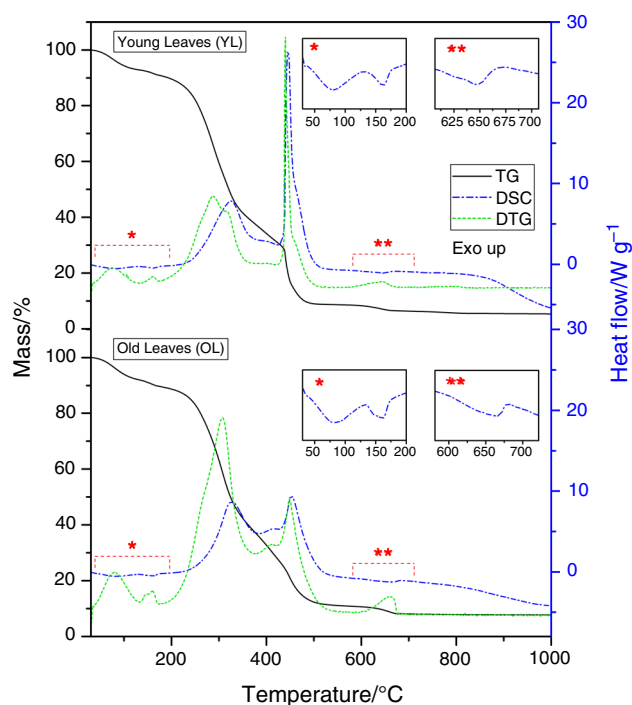


Fig. 1 TG–DSC curves of *N. multiglandulosa* young (YL) and old (OL) leaves powder. Heating rate of 10 °C min⁻¹, 70 μ L alumina pans, 10 mg samples and air purge gas at 50 mL min⁻¹ flow rate

The thermal decomposition of the leaves organic matter occurs through two consecutive and/or overlapped steps of mass loss for both YL and OL, namely third and fourth steps.

The third mass loss occurs from 172 to 375 °C (YL, 53.27%) and 173–374 °C (OL, 52.10%). Both are associated with an exothermic peak in DSC curve (325 °C—YL, and 327 °C—OL) and are probably attributed to the oxidation of the organic matter of the leaves, especially cellulose.

The fourth mass loss occurs from 375 to 530 °C (YL, 29.01%) and from 374 to 550 °C (26.54%). Even though the mass losses are similar, the TG–DSC curves profiles for this step differ in the samples. For the YL it begins with a slow mass loss, with a small exothermic event in the DSC curve (~ 405 °C). Consecutively, a fast and highly energetic decomposition process with exothermic peak at 445 °C (with a shoulder at 467 °C) occurs. This process is probably due to the combustion of the carbonaceous residue formed during the thermal decomposition of the organic matter. For the OL the same process occurs with an exothermic event at ~ 405 °C, and consecutively a slower mass loss process is observed, with a less exothermic event in the DSC curve with peak at 452 °C.

The last mass loss, from 580 to 840 °C (YL, 3.20%) and from 550 to 800 °C (OL, 3.25%), can be attributed to the decomposition of a carbonate derivative (probably calcium), associated with a small endotherm between 570 to 678 °C (YL) and 593 to 678 °C (OL).

Finally, the residue left after the heating until 1000 °C was visually inspected. For the OL sample, the residue showed a red color, which was attributed to the presence of iron(III) oxide (Fe_2O_3), once this metal is present in a substantial amount in plant tissues [8]. A qualitative test with potassium thiocyanate solution was performed after dissolution of the residue in concentrated hydrochloric acid. The appearance of a deep red color confirmed the presence of iron(III) cations.

For the YL sample, the residue showed a grayish color, which is probably due to the formation of calcium or magnesium oxide, among other typical oxides. By the residue, we can conclude that the ash content for YL and OL samples is 5.56 and 7.86%, respectively.

Young and old leaves methanolic extracts

In Fig. 2 it is represented the young leaves (YLME) and old leaves (OLME) methanolic extracts TG–DSC curves. It can be noted that these curves show a similar profile up to approximately 500 °C. The main difference between the samples is the fast mass loss around 550 °C in the OL sample, which is probably associated with its greater content of tannins (a class of compounds responsible for

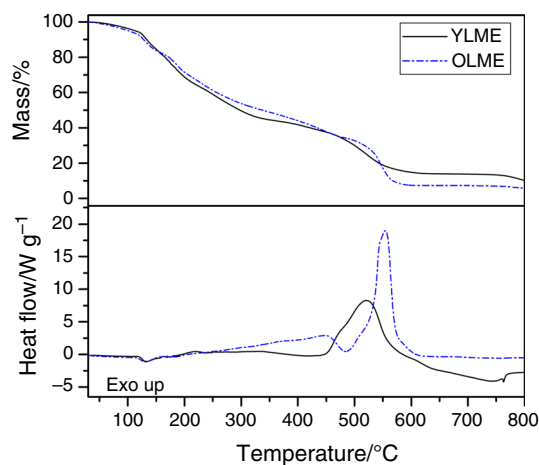


Fig. 2 Simultaneous TG–DSC curves of *N. multiglandulosa* young (YLME) and old leaves (OLME) methanolic extracts. Heating rate of 10 °C min^{-1} , 70 μL alumina pans, 10 mg samples and air purge gas at 50 mL min^{-1} flow rate

providing defense and protection for the plant against UV radiation [9]), accordingly with ongoing (unpublished) studies involving this plant. The simultaneous DSC curve show a highly exothermic peak at 555 °C associated with this mass loss, while in the YLME DSC curve a smaller exothermic peak at 521 °C is observed.

The endothermic peak observed at 762 °C in the YLME DSC curve could be attributed to a phase transition or fusion of a possible intermediate formed during thermal degradation that was not identified in this study.

Differential scanning calorimetry (DSC)

Only the powder samples were analyzed by DSC once the main objective was to evaluate the differences in water content and hydration behavior of the leaves. The cyclic DSC curves of YL powder sample is presented in Fig. 3. The OL sample will not be discussed in detail due to its similar behavior. It can be seen in the curve the similar profile of dehydration that occurs in two steps up to 180 °C, as discussed previously in the TG–DSC section.

After heating the sample up to 180 °C during the cooling cycle an endothermic event at 148 °C is observed. Even though the atmospheric compressed air used was dried, we believe that some residual humidity persists, which causes the endothermic phenomenon described. The water affinity of the sample is probably associated with the large number of OH groups present in the cellulose molecule structure, which can form strong hydrogen bonds with water molecules from the atmosphere. This agrees with a previous study that asses to be very difficult to obtain cellulose in its absolute dry state [10].

To confirm this finding, a cyclic (heating/cooling/heating) TG analysis from YL was performed. The results are

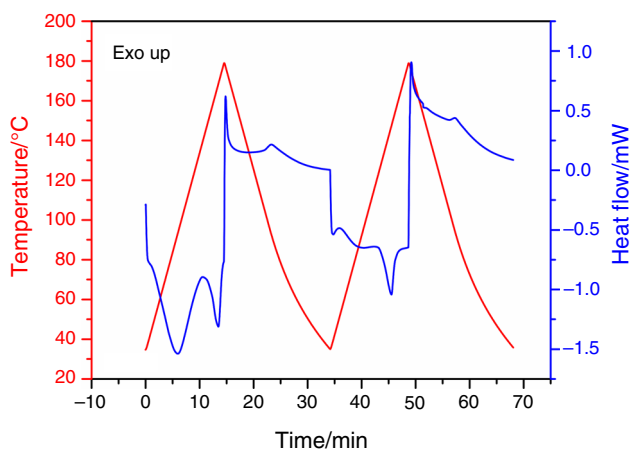


Fig. 3 Cyclic (heating/cooling/heating) DSC curve for young leaves (YL) powder sample. Heating/cooling rate of $10\text{ }^{\circ}\text{C min}^{-1}$, pierced lid aluminum pans, 2.0 mg samples, air purge gas at 50 mL min^{-1} flow rate

shown in Fig. 4. As can be seen, after dehydration on the first heating cycle, the sample gains weight when cooled. On the second heating cycle, the sample loses mass again. These are good evidence to confirm that the endothermic event observed on the second heating on DSC cyclic curve is due to the dehydration, and evidence the instability of anhydrous cellulose, even under minimum humidity atmosphere.

Infrared absorption spectroscopy

The milled leaves and methanolic extracts samples were also analyzed by means of infrared spectroscopy employing attenuated total reflectance technique, and Fig. 5 shows the spectra for both samples. As cellulose is one of the

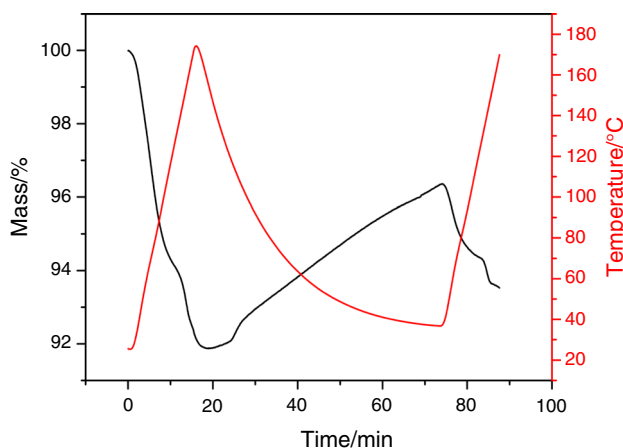


Fig. 4 Cyclic (heating/cooling/heating) TG curve for the YL powder sample. Heating rate of $10\text{ }^{\circ}\text{C min}^{-1}$, $70\text{ }\mu\text{L}$ alumina pans, 10 mg samples and air purge gas at 50 mL min^{-1} flow rate

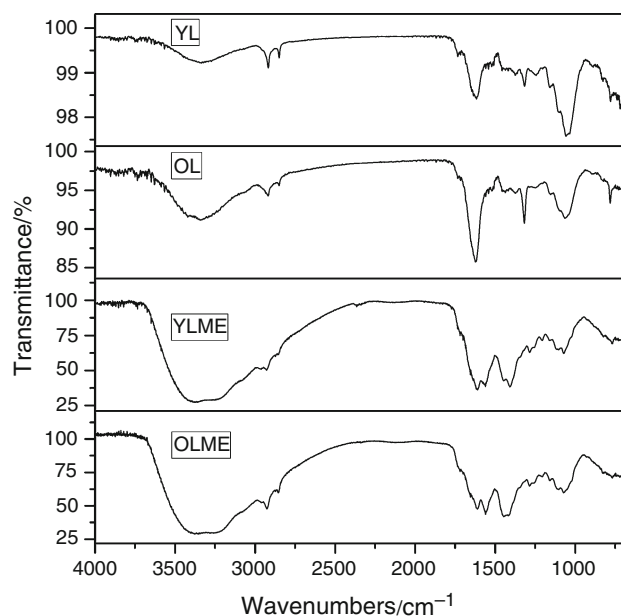


Fig. 5 Infrared spectrum of *N. multiglandulosa* young leaves (YL), old leaves (OL), and its methanolic extracts (YLME, OLME) samples

most abundant constituent in plant leaves, the most bands observed in the spectra are attributed to cellulose. The broad band from $3000\text{ to }3500\text{ cm}^{-1}$ is characteristic of hydrogen bonded $\nu\text{O-H}$ stretching vibration. The 1060 cm^{-1} absorption was attributed to $\nu\text{C-O}$ stretching mode. The absorption in 2919 and 2853 cm^{-1} was attributed to aliphatic νCH_2 symmetric and antisymmetric stretching, respectively [11].

For the extract samples the FTIR spectra show bands that correspond well to tannin spectra found in the literature [12]. The broad band around 3300 cm^{-1} can be attributed to OH stretching absorption from the phenolic and polar groups in general, which was expected to be observed in this polar extract. C-H stretching vibrational mode is present in $\sim 2927\text{ cm}^{-1}$. The bands present in the range of $1700\text{--}1400\text{ cm}^{-1}$ were attributed to carbon-carbon aromatic ring stretching modes, in which the absorption peak in 1445 cm^{-1} is the most intense one. Despite some small differences in the intensity of bands, the FTIR spectra of both samples did not evidence any difference in the composition of the YL and YLME samples when compared to the OL and OLME samples.

Evolved gas analysis

The evolved gaseous products spectrum acquired for YL and OL powder samples is shown in Fig. 6, while the infrared spectrum obtained for YLME is shown in Fig. 7. In this case, the OLME will not be discussed due to the similar gases evolved compared to YLME. These spectra

Fig. 6 Infrared spectrum from the gaseous products released at 27 and 24 min of analysis for OL and YL powder samples, respectively, associated with the third mass loss step in TG curve (225–356 °C)

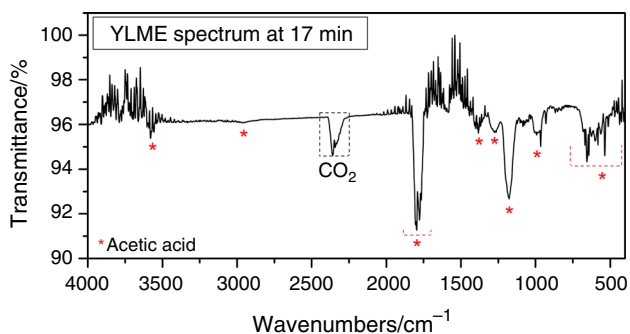
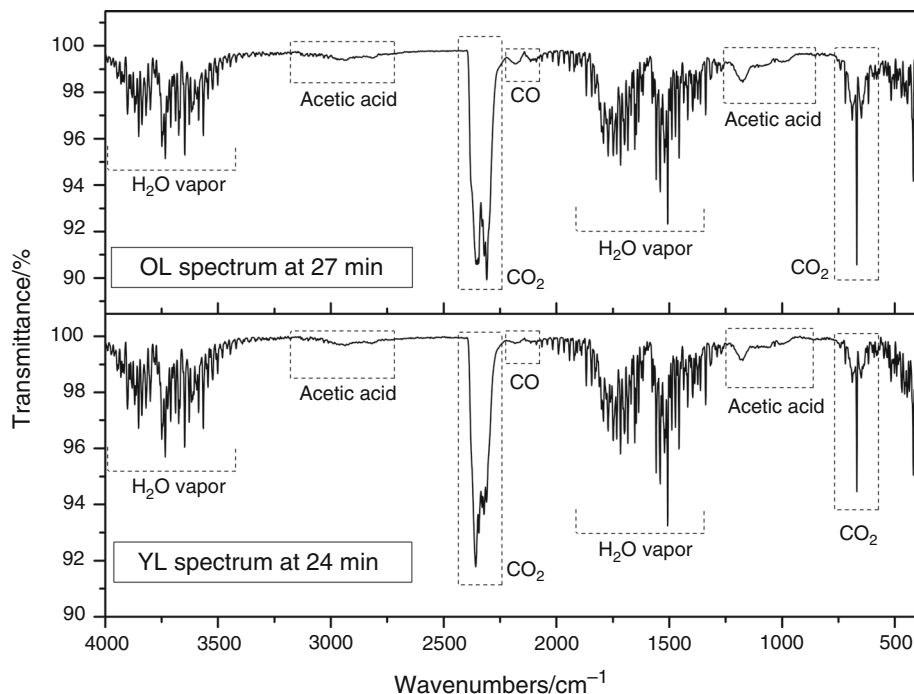


Fig. 7 Infrared spectrum from the gaseous products released at 17 min of analysis (temperature range of 170–200 °C in TG curve). This spectrum corresponds to the acetic acid vapor absorption bands with 81.85% correlation (Thermo Fisher Scientific, Omnic Software, ver. 8.0.0.322, EPA Vapor Phase library)

represent the main gases evolved (water vapor, CO₂, CO and acetic acid) during thermal decomposition of samples.

For the powder samples (Fig. 6) it can be seen a greater release of CO₂ compared to the extract (Fig. 7). The spectra collected at 27 min (OL) and 24 min (YL) (Fig. 6) are representative for the gaseous species released in the temperature range of approximately 225–356 °C, in which the third mass loss occurs for both samples, and where the major oxidative decomposition occurs. This step may be attributed to oxidative degradation of cellulose/hemicellulose and other major constituents present in powder samples, which is absent in the extract. Despite the oxidative conditions (air atmosphere) that were employed, these are common products released during pyrolysis of vegetal

material, as woods and plant leaves. The acetic acid is generated mainly due to the decomposition of hemicellulose acetyl groups [13], a complex saccharide and one of the major constituents of cell walls.

In the YLME, the major constituent at 17 min of analysis is acetic acid vapor (bands indicated by stars in Fig. 7). This spectrum is representative of the gases evolved within the temperature range of 170–200 °C in which a slow mass loss step begins for both samples (YLME and OLME). In this case, the greater concentration of acetic acid vapor compared to powder samples could be attributed to carboxylated compounds that may be concentrated in the extract, probably the major precursors for this gaseous species upon thermal degradation. Nevertheless, further studies of separation, identification and quantification of the compounds present in the extracts are necessary to confirm this hypothesis.

Conclusions

The TG–DSC profile of powder and extract samples are slightly different. However, the DTG curve profile can be more useful for identification since it is characteristic for each sample. Also, the color of the residue obtained when the powder samples are heated up to 1000 °C in air atmosphere is different for each one. These differences could be useful for differentiate between old and young leaves.

The cyclic DSC and TG profiles showed the reversibility of dehydration for powder samples. The sample dehydrates when heated, and gains mass when cooled. In a second heating cycle the samples lose mass again and an endothermic peak can be observed in the same temperature range. Even though dried air atmosphere was used as purge gas, we believe that some residual humidity persists, and once a great content of cellulose is expected in the powder sample, it rehydrates when cooled. This finding agrees with the well-known hygroscopicity of cellulose, and some studies reported in the literature.

From FTIR analysis both samples present similar absorption spectra. The powder sample presents bands characteristic of cellulose, which probably is the most abundant constituent in this samples. Both young and old leaves methanolic extracts also show very similar spectra, characteristic of tannins, although other molecules' functional groups may contribute to the observed absorption spectra.

The EGA spectra show that the samples' main decomposition products are H₂O vapor, CO₂, CO and acetic acid vapor, the latter being more abundant in YLME.

Although some hypotheses were raised concerning the thermal behavior of such samples, as well as the main constituents based on the infrared absorption spectra of the samples, a more detailed study is necessary to obtain a deep understanding of the cause of these differences.

Acknowledgements The authors acknowledge CAPES, CNPq (Project No. 421469/2016-1) INCT-CNPq (Project No. 2014/465637-0), INCT-FAPESP (Project No. 2014/50926-0), CEPID-FAPESP (Project No. 2013/07600-3) and FAPESP (Project No. 2017/14936-9) agencies for financial support. The authors are thankful to Prof. Dr. Nilton Carvalho and Prof. Dr. Ricardo Lemos for the collection of *N. multiglandulosa*. HMR acknowledges scholarship #152341/2015-2 from CNPq.

References

1. Anderson WR. Eight segregates from the neotropical genus *Mascagnia* (Malpighiaceae). *Novon*. 2006;16:168–204.

2. Riet-Correa F, Medeiros RMT, Schild AL. A review of poisonous plants that cause reproductive failure and malformations in the ruminants of Brazil. *J Appl Toxicol*. 2012;32:245–54.
3. Carvalho NM, Alonso LA, Cunha TG, Ravedutti J, Barros CSL. Intoxicação de bovinos por *Tetrapteryx multiglandulosa* (Malpighiaceae) em Mato Grosso do Sul. *Pesqui Veterinária Bras*. 2006;26:139–46.
4. Wesołowski M, Koniecznyński P. Thermal decomposition and elemental composition of medicinal plant materials—leaves and flowers. *Thermochim Acta*. 2003;397:171–80. [https://doi.org/10.1016/S0040-6031\(02\)00319-2](https://doi.org/10.1016/S0040-6031(02)00319-2).
5. Fernandes FHA, Santana CP, Santos RL, Correia LP, Conceição MM, Macêdo RO, et al. Thermal characterization of dried extract of medicinal plant by DSC and analytical techniques. *J Therm Anal Calorim*. 2013;113:443–7.
6. Correia LP, de Santana CP, da Silva KMA, de Ramos Júnior FJL, Lima RSC, de Souza FS, et al. Physical and chemical characteristics of *Maytenus rigida* in different particle sizes using SEM/EDS, TG/DTA and pyrolysis GC–MS. *J Therm Anal Calorim*. 2016. <https://doi.org/10.1007/s10973-016-5999-0>.
7. Ferreira LMB, Kobelnik M, Regasini LO, Dutra LA, da Silva Bolzani V, Ribeiro CA. Synthesis and evaluation of the thermal behavior of flavonoids: thermal decomposition of flavanone and 6-hydroxyflavanone. *J Therm Anal Calorim*. 2017;127:1605–10.
8. Farago ME, editor. *Plants and the chemical elements: biochemistry, uptake, tolerance and toxicity*. Weinheim, Germany: Wiley-VCH; 1994. <https://doi.org/10.1002/9783527615919>.
9. Brillouet JM, Romieu C, Schoefs B, Solymosi K, Cheynier V, Fulcrand H, et al. The tannosome is an organelle forming condensed tannins in the chlorophyllous organs of Tracheophyta. *Ann Bot*. 2013;112:1003–14.
10. Szcześniak L, Rachocki A, Tritt-Goc J. Glass transition temperature and thermal decomposition of cellulose powder. *Cellulose*. 2008;15:445–51.
11. Ciolacu D, Ciolacu F, Popa VI. Amorphous cellulose—structure and characterization. *Cellul Chem Technol*. 2011;45:13–1. [http://www.cellulosechemtechnol.ro/pdf/CCT1-2\(2011\)/p.13-21.pdf](http://www.cellulosechemtechnol.ro/pdf/CCT1-2(2011)/p.13-21.pdf).
12. Lisperguer J, Saravia Y, Vergara E. Structure and thermal behavior of tannins from *Acacia dealbata* bark and their reactivity toward formaldehyde. *J Chil Chem Soc*. 2016;61:3188–90.
13. Güllü D, Demirbaş A. Biomass to methanol via pyrolysis process. *Energy Convers Manag*. 2001;42:1349–56. [https://doi.org/10.1016/S0196-8904\(00\)00126-6](https://doi.org/10.1016/S0196-8904(00)00126-6).